Nucleotide-Free Actin: Stabilization by Sucrose and Nucleotide Binding Kinetics†

Enrique M. De La Cruz and Thomas D. Pollard*

Department of Cell Biology and Anatomy, The Johns Hopkins University School of Medicine, 725 North Wolfe Street, Baltimore, Maryland 21205

Received November 7, 1994; Revised Manuscript Received February 7, 1995®

ABSTRACT: We prepared nucleotide-free actin in buffer containing 48% (w/v) sucrose. Sucrose inhibits the irreversible denaturation of actin that follows nucleotide dissociation [Kasai *et al.* (1965) *Biochim. Biophys. Acta 94*, 494−503]. Our conditions removed nucleotide from ~80% of the actin. Stabilization of nucleotide-free actin depends on the sucrose concentration. The CD ellipticity ($\times 10^3$ deg cm^2 dmol^{-1}) at 222 nm of nucleotide-free actin in 48% sucrose is −3.54. The ellipticity of denatured nucleotide-free actin in dilute buffer is −2.01 and that of native actin is −4.19. In 48% sucrose nucleotide-free actin has 1.12 and native actin has 0.5 solvent-exposed thiol residues. The conformation of native actin is recovered when ATP and Mg^{2+} are added. Our ability to generate stable nucleotide-free actin permitted us to study the kinetics of nucleotide binding to actin. The observed rate constant of the reaction is linearly dependent on the concentration of ϵATP, a fluorescent analog of ATP. The inverse of the association rate constant is proportional to the viscosity of the solvent with an intercept near the origin as expected for a diffusion-limited reaction. The second-order association rate constant for Mg^{2+}-ATP and Ca^{2+}-ATP binding to nucleotide-free actin in water at 22 °C is 5×10^6 M^{-1} s^{-1}. The Smoluchowski collision rate constant for actin and ATP is calculated to be 6.5×10^9 M^{-1} s^{-1}, which makes the "orientation factor" 7.7×10^{-4}. From the ratio of the dissociation and association rate constants, we calculate dissociation equilibrium constants of 1.2×10^{-9} M for Mg^{2+}-ATP−actin, 4.4×10^{-9} M for Mg^{2+}-ϵATP−actin, and 1.2×10^{-10} M for Ca^{2+}-ATP−actin.

Actin monomers tightly bind a nucleotide, ATP[1] or ADP, and a divalent cation, Mg^{2+} or Ca^{2+}. The divalent cation is directly coordinated by the β- and γ-phosphates of ATP (Valentin-Ranc & Carlier, 1989; Kabsch *et al.*, 1990). Nucleotide binding is highly dependent on the divalent cation, such that removing the bound cation with EDTA decreases the affinity of actin for ATP by at least 4 orders of magnitude (Valentin-Ranc & Carlier, 1991; Kinosian *et al.*, 1993). Actin rapidly and irreversibly denatures if the bound nucleotide and divalent cation are removed in dilute buffers (Asakura, 1961; Kasai *et al.*, 1965; Lehrer & Kerwar, 1972; Nagy & Strzelecka-Golaszewska, 1972; Strzelecka-Golaszewska *et al.*, 1985). However, Kasai *et al.* (1965) discovered that nucleotide and divalent cation removal is reversible in high concentrations of glycerol or sucrose.

The nucleotide and divalent cation bound to actin greatly affect the kinetics and thermodynamics of actin polymerization [for review and references, see Sheterline and Sparrow (1993)]. To understand the physical basis for this regulation, the kinetic mechanisms of nucleotide and divalent cation binding to actin must be completely understood. Extensive research on the binding of Ca^{2+} and Mg^{2+} demonstrates that the association rate constant of Ca^{2+} binding to ATP−actin ($k_+ = 20 \times 10^6$ M^{-1} s^{-1}) is about 100 times faster than Mg^{2+}, and the dissociation rate constant of Ca^{2+} ($k_- = 0.015$ s^{-1}) is about 10 times more rapid (Kinosian *et al.*, 1993; Estes *et al.*, 1992). The dissociation rate constants of ATP (Table 1) and ADP (Kinosian *et al.*, 1993; Pollard *et al.*, 1992; Frieden & Patane, 1988; Neidl & Engel, 1979) have been determined under many different conditions.

Although most of the reactions of actin with nucleotides and divalent cations are well-defined, questions remain about the association rate constant for nucleotide binding to actin. The experiment is challenging because nucleotide-free actin denatures rapidly at a rate of 0.2 s^{-1} (Kinosian *et al.*, 1993). Waechter and Engel (1977) and Nowak and Goody (1988) circumvented the problem with double mixing experiments to measure the rate of nucleotide binding. During a brief pretreatment with 1 mM EDTA for 7 (Nowak & Goody, 1988) or 20 s (Waechter & Engel, 1977), the bound divalent cation and nucleotide dissociated. Both groups measured a nucleotide dissociation rate constant of 0.14 s^{-1} in 1 mM EDTA. Inevitably, part of the nucleotide-free actin also denatured during the pretreatment. From the rate constants for nucleotide dissociation and denaturation, we calculate that 7 s after addition of EDTA the sample consists of 40% ATP−actin, 29% nucleotide-free actin, and 31% denatured actin. Therefore, more than 70% of the actin in the experiments of Nowak and Goody (1988) was incapable of binding nucleotide and contributing to the kinetic analysis. After being mixed with Ca^{2+} and ϵATP, the nucleotide rebound to actin. Both groups estimated the association rate constant to be ~6×10^6 M^{-1} s^{-1} in 0.7−0.8 mM $CaCl_2$.

We hoped that the analysis of nucleotide binding to actin would be simplified if we could prepare stable nucleotide-free actin. Fortunately, Kasai *et al.* (1965) had reported that

† This work was supported by NIH Research Grant GM26338 to T.D.P. and an NSF Predoctoral Fellowship Award to E.M.D.L.C.

* To whom correspondence should be addressed [telephone, (410) 955-5664; Fax, (410) 955-4129; E-mail, Pollard@jhuigf.med.jhu.edu].

® Abstract published in *Advance ACS Abstracts,* April 1, 1995.

[1] Abbreviations: ATP, adenosine 5′-triphosphate; ϵATP, 1,N^6-ethenoadenosine 5′-triphosphate; reconstituted actin, nucleotide-free actin reconstituted with ATP and Mg^{2+}; EDTA, ethylenediaminetetraacetic acid; EGTA, ethylene glycol bis(β-aminoethyl ether)-*N,N,N′,N′*-tetraacetic acid; CD, circular dichroism; DTNB, 5,5′-dithiobis(2-nitrobenzoic acid).

0006-2960/95/0434-5452$09.00/0

sucrose inhibits the irreversible denaturation of nucleotide-free actin. We confirmed their observations and characterized the physical properties of nucleotide-free actin. This actin preparation allowed us to reinvestigate the transient kinetics of ϵATP, a fluorescent analog of ATP, binding to nucleotide-free actin. The binding reaction is diffusion-limited, but the association rate constant is relatively low, suggesting that the nucleotide binding site is not readily accessible.

MATERIALS AND METHODS

Reagents. Salts, buffers, fluorescent grade imidazole, ethylenediaminetetraacetic acid (EDTA), ethylene glycol bis-(β-aminoethyl ether)-*N,N,N',N'*-tetraacetic acid (EGTA), 5,5'-dithiobis(2-nitrobenzoic acid) (DTNB), NaN_3, L-cysteine, Dowex 1, and grade I adenosine 5'-triphosphate (ATP) were obtained from Sigma Chemical Co. (St. Louis, MO). Sephadex G-25 (coarse) was from Pharmacia (Piscataway, NJ). Sucrose and urea (ultrapure) were obtained from GIBCO BRL (Gaithersburg, MD). Dithiothreitol was from Boehringer Mannheim Corp. (Indianapolis, IN). New England Nuclear (Boston, MA) provided [α-^{32}P]ATP. Pyrenyliodoacetamide, 1,N^6-ethenoadenosine 5'-triphosphate (ϵATP), and Calcium Green-1 came from Molecular Probes (Eugene, OR). The purity of ϵATP (96%) was assessed using ascending thin-layer chromatography on PEI−cellulose with 1.0 M LiCl (Randerath & Randerath, 1967), Mono-Q FPLC (Pharmacia), and matrix-assisted laser desorption time-of-flight (MALDI-TOF) mass spectrometry (Cotter, 1992).

Protein Purification and Modification. Actin was purified from rabbit skeletal back and leg muscles by the method of Spudich and Watt (1971) and stored as Ca^{2+}-actin in continuous dialysis at 4 °C against buffer A (0.2 mM ATP, 0.5 mM DTT, 0.1 mM $CaCl_2$, 1 mM NaN_3, 2 mM Tris, pH 8.0). Actin concentration was determined by absorbance at 290 nm using a molar extinction coefficient of 2.66×10^4 M^{-1} cm^{-1}. Pyrene-labeled actin was prepared as described (Pollard, 1984) and was used at 5% of the total actin concentration. Actin containing bound Mg^{2+} was made by adding 200 μM EGTA and 80 μM $MgCl_2$ to Ca^{2+}-actin in buffer A. Actin containing bound Mg^{2+} and ϵATP (Waechter & Engel, 1975) was made by incubating actin with 200 μM ϵATP, 0 ATP, 80 μM $MgCl_2$, and 200 μM EGTA at 4 °C for at least 4 h (Pollard *et al.*, 1992). Actin with bound [α-^{32}P]ATP was made the same way except [α-^{32}P]ATP was added as a tracer with unlabeled ATP.

Preparation of Nucleotide-Free Actin. "Nucleotide-free actin" was prepared by mixing 250 μL of Mg^{2+}-actin with 750 μL of ice-cold S buffer (1 g of sucrose plus 750 μL of 20 mM Tris, pH 8.0) and adding 44 μL of 5 mM EDTA, pH 7.5, and then 100 μL of a 1:1 Dowex 1 slurry in 20 mM Tris, pH 8.0. Samples were rocked gently at 4 °C for 60 min to keep the Dowex suspended. Reactions were terminated by filtering out the Dowex resin through a 0.2-μm Millipore filter. Actin was usually diluted from a concentrated stock into 20 mM Tris, pH 8.0, prior to stripping of nucleotide to minimize the free ATP concentration in the sample. The final sucrose concentration is calculated to be 48% w/v (~1.5 M), and the final EDTA concentration is 200 μM. We used Calcium Green-1 to measure 1.4 ± 1.2 μM ($n = 6$) free Ca^{2+} remaining in solution due to a competition between metal and Dowex for EGTA. FPLC, fluorescence, A_{259}, thin-layer chromatography, and mass spectrometric analysis indicate that Dowex removes >99% of free tri- and diphosphonucleotides (ATP, ϵATP, ADP, and ϵADP) from solution under our experimental conditions (*i.e.*, 48% sucrose, pH 8.0). "Reconstituted nucleotide-free actin" samples were made 1 mM $MgCl_2$ and 1 mM ATP by adding 10 μL of 100 mM stocks into 990 μL of sample. "Control actin" is native actin containing bound nucleotide and divalent cation. For ϵATP binding experiments, control actin was treated only with Dowex for 3−5 min to remove any free ATP.

To measure the efficiency and rate of nucleotide removal, actin containing [α-^{32}P]ATP or ϵATP was used. The procedure was performed as described above except 50-μL aliquots were taken at various time points and diluted into 950-μL of stop buffer (80 μM $MgCl_2$, 200 μM EGTA, 2 mM Tris, pH 8.0). Dowex was pelleted in a microcentrifuge (16000*g* for 30 s), and 700-μL samples were either counted in a scintillation counter or fluorescence intensities (λ_{ex} = 340 nm, λ_{em} = 410 nm) were recorded on a Hitachi Perkin-Elmer 650-10S fluorescence spectrophotometer. The time course of the reaction was fitted with a nonlinear least-squares curve fitting program employing the Marquardt algorithm (Press *et al.*, 1987).

Determination of Free Metal Concentration. The free divalent cation concentration was determined with the fluorescent calcium indicator Calcium Green-1 as described by the manufacturer (Molecular Probes) using an excitation wavelength of 508 nm and an emission wavelength of 534 nm. The fluorescence of the free dye was determined in the presence of 10 mM EGTA, and the Ca^{2+}-bound fluorescence was measured in 1 mM Ca^{2+}. All measurements were made on a Photon Technology International Alphascan fluorescence spectrophotometer.

Intrinsic Fluorescence. The intrinsic fluorescence spectrum of actin was used to monitor formation of the denatured state (Lehrer & Kerwar, 1972). Fluorescence emission was scanned from 290 to 400 nm on a Photon Technology International Alphascan fluorescence spectrophotometer. Fluorescence intensities were recorded every 0.5 nm. The excitation maximum for native actin under our experimental conditions was 287 nm, and the emission maximum was 326 nm. The emission maximum for actin denatured with EDTA was 335 nm. Maxima were selected using the software supplied with the instrument. Spectra were corrected for solvent scattering. The temperature of the thermostated cuvette holder was 22 °C.

Circular Dichroism. Circular dichroism spectra were obtained at 0.5 °C with an Aviv Model 60 DS CD spectropolarimeter. A rectangular demountable cuvette made of Suprasil quartz (Hellma) with a 0.1-mm path length was used. Sample size was 50 μL. Spectra were recorded from 260 to 187 nm every 0.5 nm with an integration time of 1 s for buffer samples and 2 s for protein samples. Spectra were smoothed to a third-order polynomial function. The spectra reported represent the mean of five repeat scans. The temperature was 0.5−1.0 °C, and the actin concentration was 20 μM. Ellipticity was calculated with a molecular weight of 43 000.

Thiol Exposure. To determine solvent-exposed thiols, DTT was removed from actin in buffer A by passing through a G-25 coarse spun column. Reaction of 5,5'-dithio*bis*(2-nitrobenzoic acid) (DTNB) with solutions of actin at 22 °C

was followed spectrophotometrically at 408 nm after the reaction was initiated by adding a 10-fold excess of DTNB to actin samples essentially as described by Faulstich (Faulstich *et al.*, 1984; Drewes & Faulstich, 1991). Equivalents of reacted DTNB were determined from standard curves generated using known concentrations of L-cysteine in sucrose.

Pyrene Fluorescence Assay. Extent of actin polymerization was determined from the fluorescence intensity at 407 nm (λ_{ex} = 365 nm) of samples containing a 5% trace of pyrenylactin. Nucleotide-free actin (10.9 μM, 5% pyrenylactin) in 48% sucrose or nucleotide-free actin reconstituted with 1 mM $MgCl_2$ and 1 mM ATP in 48% sucrose was diluted 4-fold into 50 mM KCl, 10 mM imidazole (pH 7.0), and 1 mM EGTA and polymerized for 4−7 h at 22 °C. The stock polymer solution was diluted with polymerization buffer to a range of actin concentrations, sonicated briefly in a bath sonicator, and then equilibrated at 22 °C for 8−12 h before steady-state fluorescence measurements were made. The slopes of the lines above the critical concentration are proportional to the fraction of native, polymerizable actin in the samples. The final sucrose concentration was 8.8%.

The excitation and emission spectra of pyrenylactin are not affected by the sucrose concentration in the samples. Higher concentrations of sucrose (>15%) decrease the excitation sensitivity of the probe at 365 nm. Therefore, capillary viscometry was used to measure polymerization of samples containing greater than 15% sucrose.

Capillary Viscometry. Polymerization was measured with an Ostwald capillary viscometer size 150 (Cannon Instrument Co., College Park, PA) in a 15 °C water bath as described by Cooper and Pollard (1982). Sample volume was 900 μL. Viscosity is plotted as specific viscosity ($\eta_{sp} = \eta_{rel} - 1$, where $\eta_{rel} = t_{sample}/t_{buffer}$). Viscometers were calibrated for each run with buffer containing all components in the sample except actin.

Transient Kinetics. The observed rate constant (k_{obs}) for ϵATP binding to nucleotide-free actin was determined by measuring the time course of the change in fluorescence intensity at 410 nm (λ_{ex} = 340 nm) of the nucleotide (Waechter & Engel, 1975; Neidl & Engel, 1979). Measurements were made using a Photon Technology International Alphascan fluorescence spectrophotometer equipped with a Hi-Tech Model SFA-12 rapid kinetics stopped-flow accessory (Hi-Tech Scientific Ltd., Salisbury, U.K.) thermostated at 22 °C. Equal volumes of 3−6 μM nucleotide-free actin in 48% sucrose were mixed with varying concentrations of ϵATP in identical buffer containing 1 mM $MgCl_2$ or 0.2 mM $CaCl_2$. Identical results were obtained whether the divalent cation was added to the nucleotide or to actin prior to mixing. Transients were fitted to exponentials with a nonlinear least-squares curve fitting program (Press *et al.*, 1987). The initial fluorescence intensity (t = 0) was determined from the fluorescence of ϵATP in the absence of actin. The rate constants were confirmed with the kinetic simulation program HopKINSIM (Wachsstock & Pollard, 1994) using the concentrations of ϵATP and nucleotide-free actin in the sample. The pH was adjusted using 100 mM buffer in the ϵATP: MES for pH 6.0, MOPS for pH 7.0, or Tris for pH 8.0. The concentration of nucleotide-free actin was calculated from the observed 80% recovery of the native state (see Results section). Control actin containing bound nucleotide was treated with Dowex to remove free nucleotides not bound to actin.

The viscosity dependence of k_{obs} for ϵATP binding to nucleotide-free actin was determined by rapidly mixing equal volumes of 6 μM nucleotide-free actin in 48% sucrose buffer with 10 μM ϵATP and 1 mM $MgCl_2$ in different sucrose concentrations (0−48%) so that the final sucrose concentration was between 24% and 48%. The second-order association rate constants (k_+) were determined by nonlinear least-squares analysis and by kinetic simulation with HopKINSIM (Wachsstock & Pollard, 1994), taking into account the concentration of the reactants. The values of $1/k_+$ were calculated with k_+ in units of μM^{-1} s^{-1}. We used a low concentration of ϵATP to minimize background fluorescence and increase the signal to noise ratio. The viscosities of the samples were taken from Anderson (1970). The rates of nucleotide association are more rapid than the rate of nucleotide-free actin denaturation in 24% sucrose, so ϵATP binding is completed before any significant loss of nucleotide-free actin occurs.

Nucleotide Exchange Kinetics. The dissociation rate constant of ATP from Mg^{2+}-actin (k_{-ATP}) was measured from the fluorescence increase when 0.5 μM Mg^{2+}-ATP−actin was added to 200 μM ϵATP in 20 mM Tris (pH 8.0) and 1 mM $MgCl_2$ buffer. The time course of fluorescence increase due to ϵATP binding was fitted with a nonlinear curve fitting program. The rate-limiting step in this assay, and hence the rate that is measured, is the dissociation of bound ATP. The dissociation rate constant of ϵATP ($k_{-\epsilon ATP}$) was measured in the same way except that Mg^{2+}-ϵATP-actin was added to buffer containing 200 μM ATP, 20 mM Tris (pH 8.0), and 1 mM $MgCl_2$ and the fluorescence decay was fitted by nonlinear regression. To determine the dissociation rate constant of ATP from Ca^{2+}-actin, 1.0 μM Ca^{2+}-ATP−actin was added to 200 μM ϵATP in 20 mM Tris (pH 8.0) and 0.2 mM $CaCl_2$ buffer.

RESULTS

(1) Removal of Nucleotide from Actin. When the high-affinity divalent cation is removed from ATP−actin by EDTA, the affinity for ATP decreases from 10^{-10} to 10^{-6} M and the bound nucleotide dissociates (Kinosian *et al.*, 1993). The time course of ϵATP dissociation in 48% sucrose buffer containing 200 μM EDTA and Dowex 1 (Figure 1) can be fitted to an exponential function with a rate constant of 0.003 s^{-1}. [α-^{32}P]ATP also dissociated with first-order kinetics and a rate of 0.002 s^{-1} (data not shown). Note that this is ~50 times slower than the dissociation of nucleotide from actin in dilute buffer containing 1 mM EDTA (Waechter & Engel, 1977; Nowak & Goody, 1988). At 60 min, an equilibrium was reached with approximately 80% of the actin in the sample free of nucleotide. Prolonged treatment, up to 120 min, did not alter this equilibrium. The residual ATP−actin in the presence of EDTA and Dowex 1 results from the high-affinity binding of actin for nucleotide and divalent cations. Dowex competes with metal for EDTA so that some divalent cation remains free in solution. Using Ca^{2+} and EGTA, we measured 1.4 ± 1.2 μM (n = 6) free Ca^{2+} in the presence of Dowex. Thin-layer chromatography, FPLC, absorption at 259 nm, fluorescence, and mass spectrometry all showed that Dowex removes >99% of nucleotides from solution under our experimental conditions.

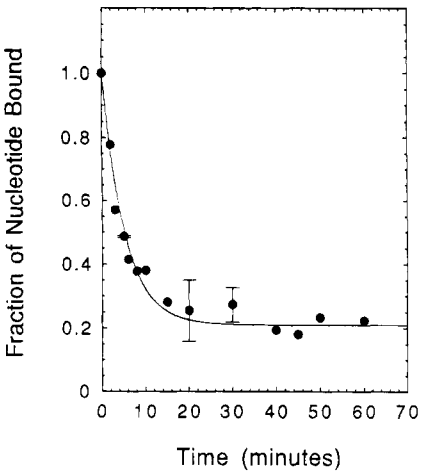

FIGURE 1: Time course of the dissociation of ϵATP from actin upon addition of EDTA and Dowex 1 in 48% sucrose. Conditions: 5 μM ϵATP−actin, 48% sucrose, 20 mM Tris (pH 8.0), 200 μM EDTA, Dowex 1, 4 °C. The fraction of actin with bound ϵATP was determined from the fluorescence intensity at 410 nm (λ_{ex} = 340 nm). The data were fitted to a single exponential with k_{obs} of 0.0033 s^{-1}. Vertical bars represent ±1 standard deviation from the mean.

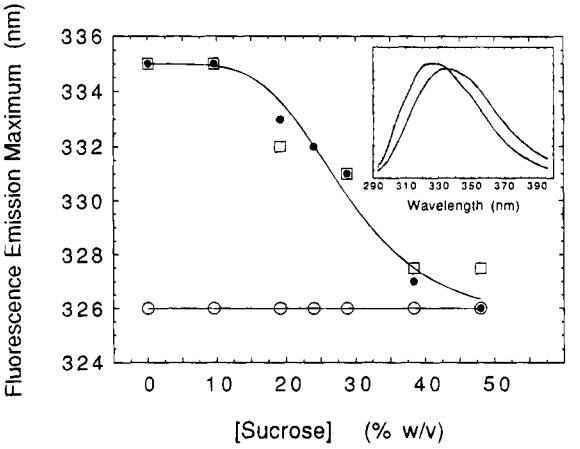

FIGURE 2: Effect of sucrose on the intrinsic fluorescence emission maximum of nucleotide-free actin, native actin, and reconstituted nucleotide-free actin. Conditions: 10.9 μM actin, 20 mM Tris (pH 8.0), 22 °C at the indicated sucrose concentrations. Symbols: (□) nucleotide-free actin; (●) nucleotide-free actin reconstituted with 1 mM ATP and 1 mM $MgCl_2$; (○) native actin in buffer containing 0.2 mM ATP and 0.1 mM $CaCl_2$. The inset shows the emission spectra of reconstituted nucleotide-free actin at 48% (left) and 0% sucrose (right).

Trace concentrations of free nucleotide remain and account for the equilibrium with 20% ATP−actin and 80% nucleotide-free actin.

(II) Sucrose Stabilizes Nucleotide-Free Actin. Our ability to generate nucleotide-free actin simplified evaluation of the kinetics of nucleotide binding (section IV below). Before considering the data, we first present evidence that nucleotide-free actin in 48% sucrose is not denatured and that the properties of native actin are regained when divalent cation and ATP rebind. This is essential, since it is well documented (Asakura, 1961; Tonomura & Yoshimura, 1961; Kasai *et al.*, 1965; Lehrer & Kerwar, 1972; Nagy & Strzelecka-Golaszewska, 1972; Strzelecka-Golaszewska *et al.*, 1985; Kinosian *et al.*, 1993) that nucleotide-free actin rapidly denatures in dilute buffers. To determine the sucrose concentration required to stabilize nucleotide-free actin, we monitored the intrinsic fluorescence of the protein over a range of sucrose concentrations. We also determined the number of solvent-exposed thiols per nucleotide-free actin monomer in 0% and 48% sucrose.

The intrinsic fluorescence emission maximum of nucleotide-free actin in dilute buffer is red-shifted from 326 to 335 nm (Figure 2) as expected for denatured actin (Lehrer & Kerwar, 1972). The red shift was reduced in high sucrose. In >40% sucrose the emission maximum of nucleotide-free actin was stable at 327.5 nm for several hours but red-shifted to 335 nm if the sucrose was diluted. The smaller red shift in >40% sucrose confirms that high concentrations of sucrose stabilize nucleotide-free actin from denaturation (Kasai *et al.*, 1965).

The sucrose dependence of the emission maximum is not due to inclusion of sucrose in the sample. First, the emission maximum of denatured nucleotide-free actin in dilute buffer remained at 335 nm when sucrose was added to 48% (data not shown). Second, sucrose, over the range of concentrations examined (0−48%), altered neither the emission (Figure 2) nor the excitation maxima of native actin.

The number of reactive thiols per nucleotide-free actin monomer also depended on sucrose (Figure 3B). In 48% sucrose, nucleotide-free actin had 1.12 reactive thiols. In dilute buffer (0% sucrose), 3.4 thiol groups of nucleotide-free actin were titrated with DTNB. Previous reports showed that nucleotide-free actin in dilute buffer has either two (Konno & Morales, 1985) or four (Faulstich *et al.*, 1984; Valentin-Ranc & Carlier, 1991) solvent-exposed thiols. Our value agrees more closely with those of Faulstich and Valentin-Ranc. Native actin in dilute buffer had 0.96 reactive thiol as reported (Faulstich *et al.*, 1984; Drewes & Faulstich, 1991) and 0.5 in 48% sucrose. In 6 M urea ~4.6 of 5 total thiols reacted with DTNB (data not shown).

In summary, sucrose concentrations ≥40% prevent the changes in the intrinsic fluorescence emission maximum (Figure 2) and the number of solvent-exposed thiol residues (Figure 3) associated with irreversible denaturation.

(III) The Conformation of Native Actin Is Recovered upon Addition of ATP and Mg^{2+} to Nucleotide-Free Actin in High Sucrose. To measure the association rate constant of the nucleotide, removal of the tightly bound nucleotide must be reversible, and the native conformation of actin must be recovered when it rebinds. In the following section we describe some physical properties of nucleotide-free actin and give evidence that it regains the native state when reconstituted with Mg^{2+} and ATP in high sucrose.

(a) Intrinsic Fluorescence. The emission maximum of nucleotide-free actin in 48% sucrose shifted from 327.5 to 326 nm when ATP and Mg^{2+} were added (Figure 2). The emission maximum was stable at 326 nm even after the sucrose was diluted. The shift in the emission to that of native actin demonstrates that binding of nucleotide and divalent cation to nucleotide-free actin in high sucrose recovers the native conformation. For nucleotide-free actin in low sucrose (<20%), the emission maximum was 335 nm even after ATP and Mg^{2+} were added. This actin did not recover its native conformation, because nucleotide-free actin denatures irreversibly in dilute buffers (Lehrer & Kerwar, 1972).

(b) Solvent-Exposed Thiols. Reconstituting ATP and Mg^{2+} lowered the number of reactive thiols of nucleotide-free actin in 48% sucrose from 1.12 to 0.65 (Figure 3A). This small

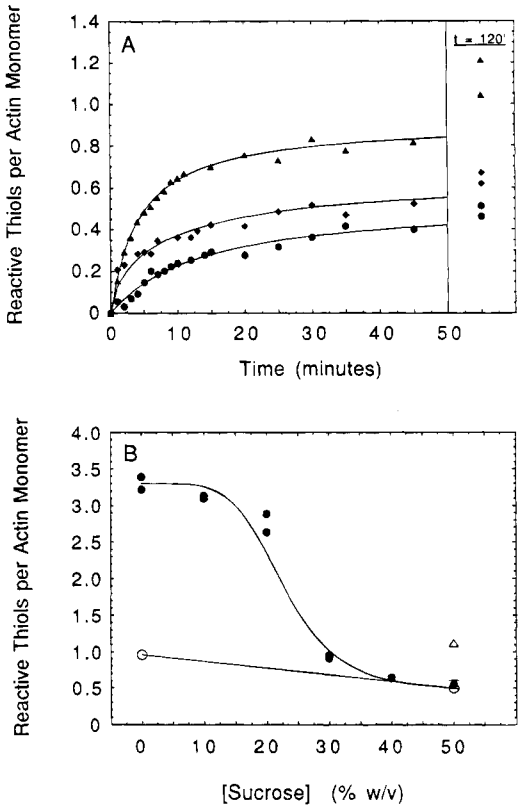

FIGURE 3: Thiol reactivity of native actin, nucleotide-free actin, and reconstituted nucleotide-free actin. (A) Time course of the reaction of DTNB with protein in 48% sucrose followed at 408 nm. Conditions: 10 μM actin, 100 μM DTNB, 48% sucrose, 20 mM Tris (pH 8.0), 22 °C. Symbols: (▲) nucleotide-free actin; (◆) nucleotide-free actin reconstituted with 1 mM ATP and 1 mM $MgCl_2$; (●) native actin in buffer containing 0.2 mM ATP and 0.1 mM $CaCl_2$. The curve through the reconstituted actin data (◆) is a theoretical time course for a mixture of 70% native actin and 30% nucleotide-free actin in 48% sucrose. (B) Dependence of the thiol reactivity of nucleotide-free actin, native actin, and reconstituted nucleotide-free actin on the sucrose concentration during nucleotide removal. Conditions: 10 μM actin, 100 μM DTNB, 20 mM Tris (pH 8.0), 22 °C at the indicated sucrose concentrations. Symbols: (△) nucleotide-free actin; (●) nucleotide-free actin reconstituted with 1 mM ATP and 1 mM $MgCl_2$; (○) native actin in buffer containing 0.2 mM ATP and 0.1 mM $CaCl_2$.

but significant difference is consistent with nucleotide-free actin in 48% sucrose recovering the native conformation when it rebinds nucleotide and divalent cation. Nucleotide-free actin in dilute buffer had 3.4 reactive thiols. Adding ATP and Mg^{2+} had no effect on the thiol accessibility (Figure 3B) as expected for denatured actin (Faulstich *et al.*, 1984).

(c) Circular Dichroism. Nucleotide-free actin in 48% sucrose has CD optical activity intermediate between native and denatured actin (Figure 4). The loss in the optical activity of nucleotide-free actin in dilute buffer (*i.e.*, denatured actin) can be explained as a partial transition of α-helical structure to a population of "unordered" species (Figure 4; Nagy & Strzelecka-Golaszewska, 1972; Strzelecka-Golaszewska *et al.*, 1985). The spectrum of nucleotide-free actin in 0% sucrose was identical before and after addition of ATP and Mg^{2+}. Nucleotide-free actin in 48% sucrose appears to have secondary structure content intermediate between native and denatured actin (Figure 4). The ellipticity at 222 nm of nucleotide-free actin in 48% sucrose is -3.54×10^3 deg cm^2 dmol^{-1}. The ellipticity of nucleotide-free actin in dilute buffer is -2.01×10^3 deg cm^2 dmol^{-1}, and that of native actin is -4.19×10^3 deg cm^2 dmol^{-1}. The ellipticity at 222 nm (θ_{222}) of nucleotide-free actin in 48% sucrose is closer to that of native actin than denatured actin, demonstrating that high sucrose stabilizes nucleotide-free actin from denaturation.

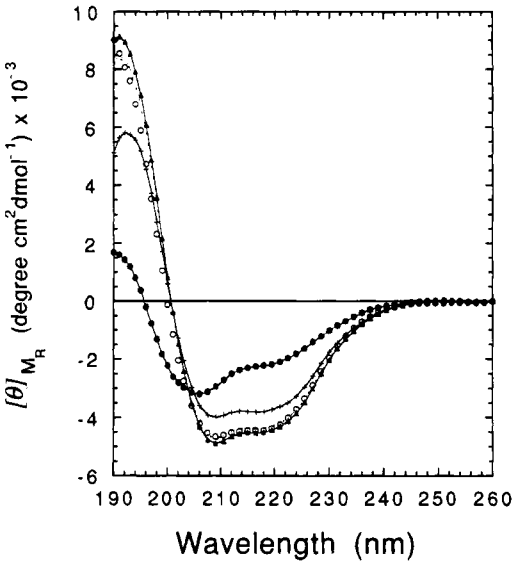

FIGURE 4: Sucrose prevents the irreversible loss of CD optical activity that occurs after removal of nucleotide and metal. Conditions: 20 μM actin, 48% sucrose, 20 mM Tris (pH 8.0), 0.5−1.0 °C. Symbols: (●) nucleotide-free actin made in the absence of sucrose; (+) nucleotide-free actin made in 48% sucrose; (○) nucleotide-free actin made in 48% sucrose reconstituted with 1 mM ATP and 1 mM $MgCl_2$; (▲) native actin in 48% sucrose. The curve through the reconstituted actin spectra (○) represents a theoretical spectra for a mixture of 80% native actin and 20% nucleotide-free actin in 48% sucrose.

Addition of ATP and Mg^{2+} to nucleotide-free actin in 48% sucrose yielded an optical activity very similar to that of native actin (Figure 4). The spectra of native actin in 0% and 48% sucrose were identical (not shown), indicating that sucrose does not perturb the secondary structure of the protein. The CD spectra of monomeric and polymerized actin in 48% sucrose were identical (data not shown), consistent with previous reports obtained in dilute buffers (Hegyi & Venyaminov, 1980). Therefore, the differences in CD optical activity are due to changes in secondary structure that result from dissociation of the bound nucleotide.

(d) Polymerization Properties of Reconstituted Actin. Polymerization of reconstituted actin depended on the sucrose concentration during nucleotide stripping. In 48% sucrose, the polymerization of nucleotide-free actin reconstituted with ATP and Mg^{2+} was approximately 80% that of native actin (Figure 5). Nucleotide-free actin prepared in 0% sucrose did not polymerize when ATP and Mg^{2+} were added. Concentrations >20% sucrose were required during stripping to allow significant polymerization after reconstitution. Polymerization decreased when greater than two thiol groups were exposed (compare Figures 3B and 5), in accord with the conclusion of Drewes and Faulstich (1991), who showed that actin with more than two solvent-exposed thiols cannot polymerize. The lower specific viscosity of native actin at high sucrose concentrations (Figure 5 inset) may be due to a decrease in filament length, but further experiments must be done to resolve this issue.

The fluorescence of pyrenylactin was used to measure polymerization after dilution of sucrose to 8.8% (Figure 6).

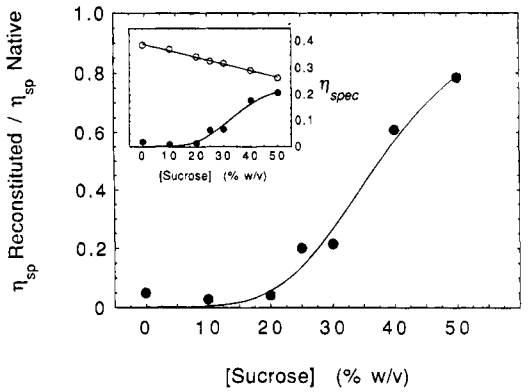

FIGURE 5: Viscosity of reconstituted nucleotide-free actin under polymerizing conditions. Conditions: 10 μM actin, 20 mM Tris (pH 8.0), 1 mM ATP, 2 mM $MgCl_2$, 50 mM KCl, 1 mM EGTA, 10 mM imidazole (pH 7.0), 25 °C at the indicated sucrose concentrations. The main plot shows the ratio of the specific viscosity of native actin to the specific viscosity of nucleotide-free actin as a function of the sucrose concentration. The inset shows the specific viscosity of control actin (○) and reconstituted nucleotide-free actin (●) as a function of the sucrose concentration.

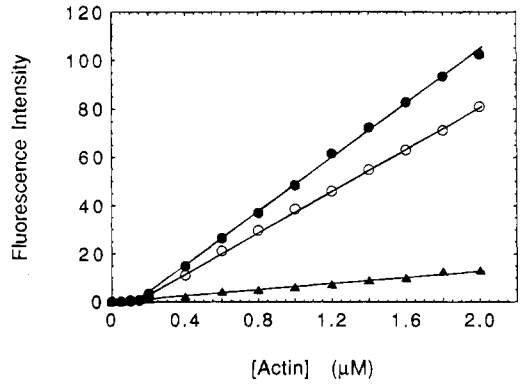

FIGURE 6: Polymerization measured by pyrene fluorescence of native actin, nucleotide-free actin, and reconstituted nucleotide-free actin. Conditions: 8.8% sucrose, 50 mM KCl, 1 mM EGTA, 10 mM imidazole (pH 7.0), 22 °C. Symbols: (▲) nucleotide-free actin; (○) nucleotide-free actin reconstituted with 1 mM ATP and 2 mM $MgCl_2$; (●) native actin containing 1 mM ATP and 2 mM $MgCl_2$.

The polymerization of reconstituted nucleotide-free actin was 80.2 ± 3.7% (n = 9) that of native actin, suggesting that ~80% of nucleotide-free actin returns to the stable, native state when nucleotide and divalent cation are added. Only 11.7 ± 1.3% (n = 4) of nucleotide-free actin without added nucleotide polymerized in the assembly buffer with 8.8% sucrose. This population may represent the residual ATP–actin in the nucleotide-free actin preparation (see Figure 1).

Consistent with an ~80% recovery of native actin, we found that the CD spectra of reconstituted actin (Figure 4) can be fitted with a theoretical spectra for a mixture of 80% native actin and 20% nucleotide-free actin. The titration of reconstituted actin's thiols (Figure 3A) is fitted to a mixture of 70% native actin and 30% nucleotide-free actin.

Taken together, the data suggest that nucleotide-free actin in 48% sucrose exists in a unique conformation different from that of native and denatured actin. It has secondary structure, thiol accessibility, and intrinsic fluorescence properties more like native actin than denatured actin. Addition of nucleotide and divalent cation recovers many physical properties (intrinsic fluorescence, thiol accessibility, CD optical activity, and polymerization) of native actin in ~80% of the sample.

(IV) Transient Kinetics of ϵATP Binding to Nucleotide-Free Actin. The fluorescence increase following mixing of Mg^{2+}-ϵATP with nucleotide-free actin in 48% sucrose follows a single exponential (Figure 7A). The time course is the same in 0.2 mM Ca^{2+}. The k_{obs} depends linearly on the ϵATP concentration over a wide range (Figure 7B,C), yielding the second-order rate constants (k_+) for the association reactions from the slope of the line. They are 0.78 × 10^6 M^{-1} s^{-1} in the presence of either Mg^{2+} or Ca^{2+}. On the time scale of seconds there is no fluorescence transient when ϵATP is mixed with actin containing bound ATP (Figure 7A). We used the fits to single exponentials to calculate the k_{obs} of the reactions even though pseudo-first-order conditions do not exist at the lower ϵATP concentrations. The transients fit single exponentials surprisingly well (R^2 ≥ 0.998 for all transients examined). This approach introduced minimal errors, because kinetic simulations using the measured k_+ and taking the concentrations of both reactants into account agree closely with the experimental data. Even a 2-fold change in k_+ yields simulations that fail to fit the experimental data (Figure 7A).

Combining the association rate constant of Mg^{2+}-ϵATP (0.78 × 10^6 M^{-1} s^{-1}) with the dissociation rate constant (0.003 s^{-1}, Figure 1) yields an apparent dissociation equilibrium constant (K_d) of 3.8 × 10^{-9} M for Mg^{2+}-ϵATP–actin in 48% sucrose.

As expected for a diffusion-limited reaction (Berg & von Hippel, 1985), the inverse association rate constant of ϵATP binding to nucleotide-free actin, $(k_+)^{-1}$, is linearly dependent on the viscosity (η) of the medium and intercepts near the origin (Figure 8). Extrapolating to a viscosity of 0.96 cP yields an association rate constant of 5 × 10^6 M^{-1} s^{-1} for ϵATP binding to nucleotide-free actin in water at 22 °C.

The k_{obs} of 5 μM Mg^{2+}-ϵATP binding to nucleotide-free actin in the presence of 48% sucrose is only slightly dependent on the pH: pH 6.0 (2.1 ± 0.3 s^{-1}, n = 11), pH 7.0 (4.3 ± 1.2 s^{-1}, n = 15), and pH 8.0 (2.8 ± 0.2 s^{-1}, n = 10).

The dissociation rate constant of ATP (k_{-ATP}) was measured by displacing the bound nucleotide from 0.5 μM Mg^{2+}-actin with a large molar excess of ϵATP. We obtain a value of 0.0064 s^{-1} for k_{-ATP} in 1 mM $MgCl_2$ (Table 1). Displacing bound ϵATP with a large molar excess of ATP showed $k_{-\epsilon ATP}$ to be 0.022 s^{-1}. The ratio of the dissociation and association rate constants yields a dissociation equilibrium constant (K_d) of 1.2 × 10^{-9} M for Mg^{2+}-ATP–actin and 4.4 × 10^{-9} M for Mg^{2+}-ϵATP–actin in water. The binding affinity of ϵATP for actin in the presence of Mg^{2+} is 3.6 times less than that of ATP, in close agreement with the 3–4-fold differences reported by Pollard *et al.* (1992) and Kinosian *et al.* (1993). We obtain a value of 0.0006 s^{-1} for k_{-ATP} from Ca^{2+}-actin in 0.2 mM $CaCl_2$, yielding a K_d of 1.2 × 10^{-10} M for the Ca^{2+}-ATP–actin complex in water.

DISCUSSION

(I) Properties of Nucleotide-Free Actin in Sucrose. Nucleotide binding depends on the divalent cation, so the nucleotide tends to dissociate when the divalent cation is removed with EDTA. Nucleotide-free actin in dilute buffers denatures rapidly with a rate constant of 0.2 s^{-1} (Kinosian *et al.*, 1993). Denaturation is irreversible, and the native

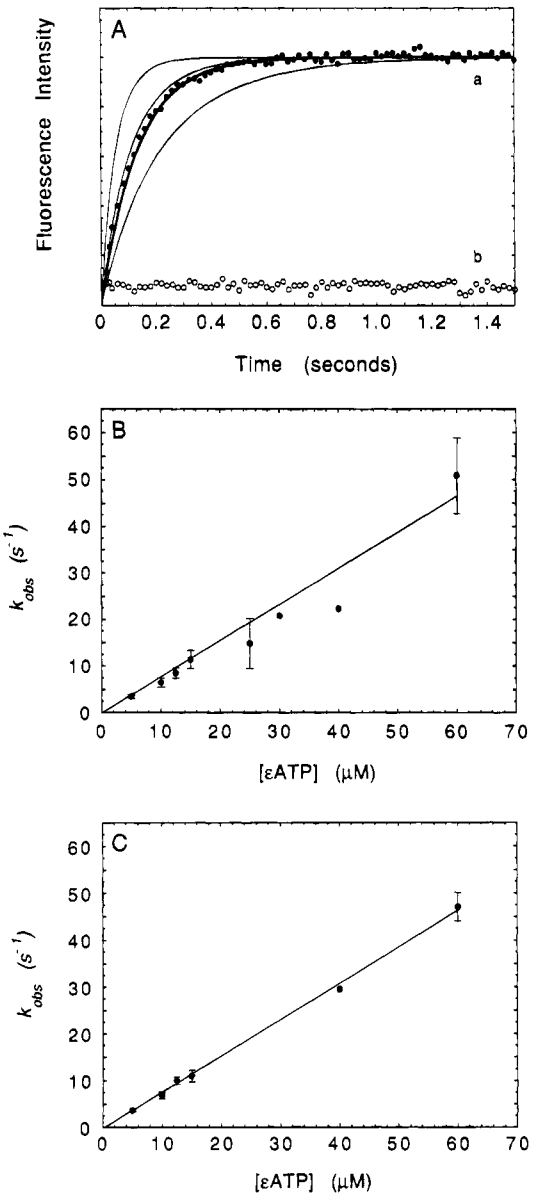

FIGURE 7: Transient kinetics of ϵATP binding to nucleotide-free actin. Fluorescence of ϵATP was monitored at 410 nm (λ_{ex} = 340 nm). (A) Curve a: 6 μM nucleotide-free actin in 48% sucrose buffer (pH 8.0) rapidly mixed with 25 μM ϵATP in 48% sucrose and 1 mM $MgCl_2$. The thick curve through the data set is the best fit to a single exponential (R = 0.999). The thin curves are kinetic simulations generated for the indicated concentrations of actin and nucleotide and the following second-order association rate constants: left, 1.56 μM^{-1} s^{-1}; middle, 0.78 μM^{-1} s^{-1}; right, 0.39 μM^{-1} s^{-1}. Curve b: 10 μM control actin in 48% sucrose buffer (pH 8.0) rapidly mixed with 25 μM ϵATP in 48% sucrose buffer containing 1 mM $MgCl_2$. (B) Dependence of the observed rate constant (k_{obs}) for association of ϵATP with nucleotide-free actin in the presence of 1 mM $MgCl_2$ on the concentration of ϵATP. (C) Dependence of the observed rate constant (k_{obs}) for association of ϵATP with nucleotide-free actin in the presence of 0.2 mM $CaCl_2$ on the concentration of ϵATP. The observed rate constants were determined from the best fits to exponentials (Press *et al.*, 1987). The second-order association rate constants (k_+) are 0.78 μM^{-1} s^{-1} in $MgCl_2$ and 0.78 μM^{-1} s^{-1} in $CaCl_2$. Bars represent $\pm$1 standard deviation from the mean (n = 3−15 for $MgCl_2$ from five different preparations, R = 0.980; n = 5−10 for $CaCl_2$ from two different preparations, R = 0.999). The final concentration of nucleotide-free actin was either 1.5, 2.5, or 3.0 μM. The origin is within experimental error of the mean of the y-intercept.

conformation cannot be recovered even with addition of excess nucleotide and divalent cation.

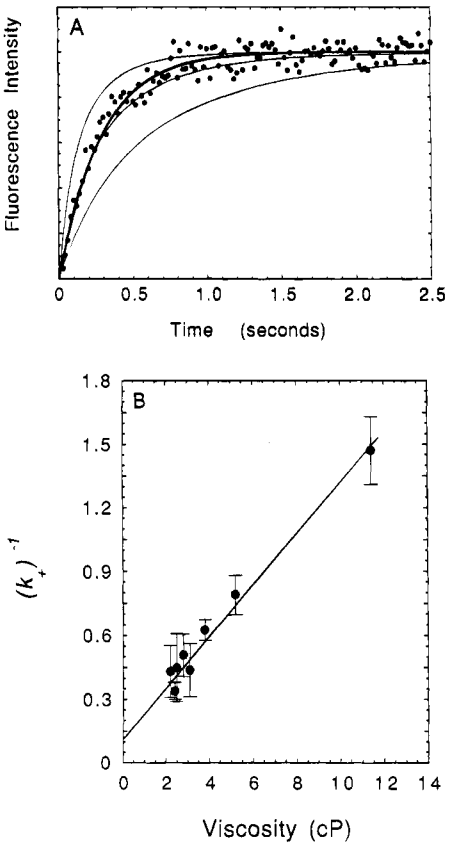

FIGURE 8: Viscosity dependence of $1/k_+$ for ϵATP binding to nucleotide-free actin. (A) Nucleotide-free actin (6 μM) in 48% sucrose buffer was rapidly mixed with 10 μM ϵATP and 1 mM $MgCl_2$ in 48% sucrose. The thick curve through the data set is the best fit to a monoexponential (R = 0.998). The thin curves are kinetic simulations generated for the indicated concentrations of actin and nucleotide and the following second-order association rate constants: left, 1.56 μM^{-1} s^{-1}; middle, 0.78 μM^{-1} s^{-1}; right, 0.39 μM^{-1} s^{-1}. (B) Nucleotide-free actin was mixed with 10 μM ϵATP and 1 mM $MgCl_2$ in a series of sucrose concentrations. The second-order association rate constants (k_+) were determined by nonlinear least-squares analysis and by kinetic simulation, taking into account the concentration of the reactants. The values of $1/k_+$ were calculated with k_+ in units of μM^{-1} s^{-1}. The temperature is 22 °C. Bars represent $\pm$1 standard deviation from the mean (n = 5−12 from two different preparations).

However, in the presence of stabilizers such as glycerol or sucrose, dissociation of the bound nucleotide is reversible (Kasai *et al.*, 1965). By several criteria (fluorescence, thiol accessibility, CD spectroscopy, and polymerization) nucleotide-free actin in 48% sucrose is much more stable than in dilute buffers and exists in a conformation different from that of native and denatured actin. Nucleotide-free actin returns to its native state when reconstituted with ATP and divalent cation. Stabilization of nucleotide-free actin and return to the native state depend on the sucrose concentration. There is no recovery in <20% sucrose. In 48% sucrose approximately 80% native actin is recovered.

The conformation of nucleotide-free actin in 48% sucrose is more like that of native than denatured actin. The intrinsic fluorescence emission maximum of nucleotide-free actin in 48% sucrose is 327.5 nm (Figure 2), very close to that of native (326 nm) but not denatured actin (335 nm). Nucleotide-free actin in 48% sucrose has approximately 1.12 solvent-exposed thiols (Figure 3). Denatured actin has 3.4 reactive thiols, and native actin in 48% sucrose has 0.5. The CD optical activity and ellipticity at 222 nm (θ_{222}) of

Table 1: Summary of Experimental Kinetic Rate Constants for ATP and ϵ-ATP Binding to Actin

nucleotide	pH	temp (°C)	[divalent cation]	k_+ (μM^{-1} s^{-1})	k_- (s^{-1})	reference
ϵ-ATP	8.2	21	0.8 mM calcium	6	0.0024	Waechter & Engel, 1977
ϵ-ATP	7.6	20	0.65 mM calcium	6.8		Nowak & Goody, 1988
ϵ-ATP	7.6	20	0.65 mM calcium	7.3	0.0005	Nowak et al., 1988
ϵ-ATP	8.2	21	0.2 mM calcium		0.0045	Waechter & Engel, 1975
ϵ-ATP	8.0	22	0.2 mM calcium	5[a]		this paper
ϵ-ATP	7.4	20	0.1 mM calcium		0.0006	Kasprzak, 1993
ϵ-ATP	8.0	20	10 μM calcium		0.006	Frieden & Patane, 1988
ϵ-ATP	7.2	22	1 μM calcium		0.026	Goldschmidt-Clemont et al., 1991
ϵ-ATP	7.0	22	0.060 μM calcium		0.020	Kinosian et al., 1993
ϵ-ATP	7.4	20	0 calcium[b]		0.028	Kasprzak, 1993
ϵ-ATP	8.0	22	1 mM magnesium	5[a]	0.022	this paper
ϵ-ATP	7.5	25	80 μM magnesium		0.015	Pollard et al., 1992
ϵ-ATP	7.5	20	50 μM magnesium		0.006	Kasprzak, 1994
ϵ-ATP	7.0	22	1 μM magnesium		0.0043	Kinosian et al., 1993
ϵ-ATP	7.6	20	0.8 mM magnesium, 100 mM KCl	2		Nowak & Goody, 1988
ATP	8.2	21	0.8 mM calcium		0.0008	Neidl & Engel, 1979
ATP	7.6	20	0.65 mM calcium	6.1		Nowak & Goody, 1988
ATP	8.0	22	0.2 mM calcium		0.0006	this paper
ATP	7.0	22	>10 μM calcium		0.0005	Kinosian et al., 1993
ATP	7.2	22	1 μM calcium		0.012	Goldschmidt-Clemont et al., 1991
ATP	7.0	22	<0.1 μM calcium		0.015	Kinosian et al., 1993
ATP	8.2	21	0 calcium[c]	0.05[d]		Nowak et al., 1988
ATP	8.0	22	1 mM magnesium		0.0064	this paper
ATP	7.0	22	>100 μM magnesium		0.0005	Kinosian et al., 1993
ATP	7.5	25	80 μM magnesium		0.0045	Pollard et al., 1992
ATP	7.5	20	50 μM magnesium		0.002	Kasprzak, 1994
ATP	7.0	22	1 μM magnesium		0.0012	Kinosian et al., 1993
ATP	7.0	22	<0.1 μM magnesium		0.0017	Kinosian et al., 1993
ATP	7.6	20	0.8 mM magnesium, 100 mM KCl	1		Nowak & Goody, 1988

[a] Extrapolated to the viscosity of water from the viscosity dependence of the association rate constant (see Figure 8). [b] Samples contained 200 μM EDTA. [c] Samples contained 1 mM EDTA. [d] Calculated from EDTA denaturation kinetics.

nucleotide-free actin in 48% sucrose (Figure 4) are closer to those of native actin than denatured actin, suggesting that nucleotide-free actin possesses secondary structure resembling native actin. Stabilization of nucleotide-free actin in a nearly native conformation appears to be essential for reversible binding of the nucleotide and recovery of the native conformation since native actin cannot be recovered in sucrose concentrations that do not stabilize nucleotide-free actin.

The mechanism of protein stabilization by sucrose has been described in terms of preferential hydration (Lee *et al.*, 1975; Lee & Timasheff, 1981) and excluded volume effects (Winzor & Wills, 1986; Ralston, 1990). Both theories predict that, in the presence of small solutes such as sucrose, the most compact state of a protein, which is usually the native state, is thermodynamically favored at equilibrium. The behavior of nucleotide-free actin is consistent with these theories. Sucrose stabilizes nucleotide-free actin in a conformation very similar to that of native actin, although the physical properties of the two states differ significantly. Nucleotide-free actin in 48% sucrose has slightly greater accessibility to thiol residues and possesses a little less secondary structure than native actin, suggesting that the stabilizing role of the bound nucleotide is to maintain the protein in a more tightly compact conformation. A similar mechanism has been proposed for stabilization of the "closed state" of hexokinase (Shoham & Steitz, 1980) and Hsc70 (Holmes *et al.*, 1993), proteins with two domains topologically similar to those of actin. In these examples, binding of ATP is believed to favor the closed conformation by increasing the number of contacts between the two domains. In the absence of ligand (*i.e.*, ATP) the opened and closed conformations are probably in rapid equilibrium [see Gerstein *et al.* (1994)]. We suggest that sucrose-stabilized nucleotide-free actin exists in a similar opened−closed rapid equilibrium. In the case of the nucleotide-free actin in sucrose, the open conformation is only slightly different from the native state. Upon binding ATP the more tightly packed, native conformation dominates.

(II) Nucleotide Binding Kinetics. The availability of stable nucleotide-free actin permitted us to investigate the kinetics of nucleotide binding using the fluorescent nucleotide analog ϵATP (Waechter & Engel, 1975; Neidl & Engel, 1979) in the presence of Mg^{2+} and Ca^{2+} and as a function of the solvent viscosity. The second-order association rate constant is independent of the divalent cation and has a value of 0.78 $\times$ 10^6 M^{-1} s^{-1} in 48% sucrose. The linear concentration dependence of k_{obs} on the [ϵATP] examined indicates that if the association reaction occurs via a two-step mechanism (*i.e.*, a rapid binding step followed by a unimolecular conformation change), the second step must occur at a rate >50 s^{-1}. The apparent binding affinity of the Mg^{2+}-ϵATP−actin complex in 48% sucrose is 3.8 $\times$ 10^{-9} M.

The viscosity dependence of the association rate constant provides strong evidence that binding of the metal−ϵATP complex is a diffusion-limited reaction with a value of 5 $\times$ 10^6 M^{-1} s^{-1} in water. Since the ratio of association rate constants for ATP and ϵATP binding to actin is 1 (Kinosian *et al.*, 1993; Nowak & Goody, 1988; Neidl & Engel, 1979), the association rate constant for metal−ATP binding to nucleotide-free actin is 5 $\times$ 10^6 M^{-1} s^{-1} as well. Similar values were measured in double-mixing experiments in Ca^{2+} by Waechter and Engel (1977) and Nowak and Goody (1988). The only disagreement is that Nowak and Goody (1988) observed a much lower association rate constant in magnesium than we have (see Table 1). The use of sucrose-

Scheme 1

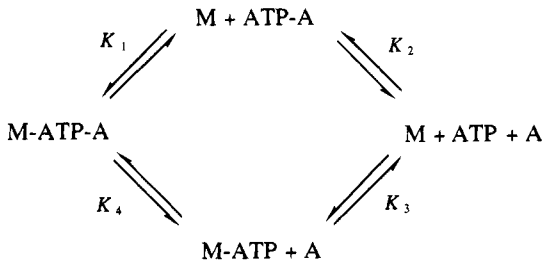

stabilized nucleotide-free actin avoids the limitations of the double-mixing experiments in dilute buffers, but it is gratifying that both methods yield similar results.

Our determined rate constants and affinities for Ca^{2+}-ATP and Mg^{2+}-ATP binding are thermodynamically consistent with the mechanism in Scheme 1 and values in the literature for other rate and equilibrium constants in dilute buffer. In Scheme 1, M is the metal, either Ca^{2+} or Mg^{2+}, and A is native actin (Valentin-Ranc & Carlier, 1989; Kinosian *et al.*, 1992). K_1 (clockwise) is 7×10^{-10} for Ca^{2+} binding to ATP−actin and 7×10^{-9} for Mg^{2+} (Gershman *et al.*, 1991; Kinosian *et al.*, 1992). K_2 is 1×10^{-6} (Kinosian *et al.*, 1992). K_3 is 2.0×10^5 for Ca^{2+} and 3.3×10^5 for Mg^{2+} binding to ATP at pH 8.0 (Frieden & Patane, 1988). We obtained a K_4 of 8.3×10^9 for Ca^{2+}-ATP−actin and 6.6×10^8 for Mg^{2+}-ATP−actin at pH 8.0.

The product of the equilibrium constants in a cyclic path should be 1. $K_1 \times K_2 \times K_3 \times K_4 = 1.2$ in the presence of Ca^{2+} and 1.5 in the presence of Mg^{2+}. Therefore, our experimentally determined values for the equilibrium, association, and dissociation rate constants in the presence of Ca^{2+} and in the presence of Mg^{2+} are thermodynamically consistent, within experimental error, with the mechanism in Scheme 1.

Theoretical values for the maximum association rate constant of a diffusion-limited reaction can be calculated from the Smoluchowski equation [see Berg and von Hippel (1985)], which defines the collision rate constant, $k_{collision}$, for two spheres diffusing randomly in solution:

$$k_{collision} = 4\pi(D_A + D_B)(r_A + r_B)N_0 10^{-3}$$

where N_0 is Avagodro's number, 10^{-3} is the ratio of liter per cm^3, D_A and D_B are the translational diffusion coefficients (in $cm^2\ s^{-1}$) for the two reacting species, and r_A and r_B are their interaction radii (in cm). Actin has a translational diffusion coefficient of $5 \times 10^{-7}\ cm^2\ s^{-1}$ (Mihashi, 1964; Lanni *et al.*, 1981; Tait & Frieden, 1982) and an interaction radius of about 1×10^{-7} cm, based on the dimensions of the nucleotide binding site in the crystal structure (Kabsch *et al.*, 1990). We calculated a radius of 4×10^{-8} cm for Mg^{2+}-ATP from the rotational correlation time (τ_r) of Mn^{2+}-ATP, $\tau_r = 1.0 \times 10^{-10}$ s (Sloan & Mildvan, 1976), with the expression

$$\tau_r = \frac{8\pi\eta r^3}{3k_B T}$$

as defined by Bloembergen and Morgan (1961). Using the Stokes−Einstein relation

$$D = \frac{k_B T}{6\pi\eta r}$$

the diffusion coefficient of Mg^{2+}-ATP in water at 22 °C was calculated to be $5.6 \times 10^{-6}\ cm^2\ s^{-1}$. These parameters give $k_{collision}$ a value of $6.5 \times 10^9\ M^{-1}\ s^{-1}$, which is about 3 orders of magnitude greater than the association rate constant of ATP binding to nucleotide-free actin in water.

The "orientation factor" takes into account the probability of the two species colliding in an orientation which leads to productive association. If every collision results in successful binding, the orientation factor is 1. In the case of ATP binding to nucleotide-free actin, the orientation factor has a value 7.7×10^{-4}. This means that approximately 1 out of every 1300 random encounters between ATP and actin results in successful binding of the nucleotide.

Although the reaction is diffusion-limited, this is a low efficiency for a small molecule binding to a macromolecule, especially when microcollisions and rotational reorientation of the nucleotide and actin are considered [see Northrup and Erickson (1992) and von Hippel and Berg (1989)]. The low probability of a successful binding collision suggests that the ATP binding site is not readily accessible. This seems plausible from a structural point of view, since the nucleotide binds in a deep cleft between the two domains of the protein (Kabsch *et al.*, 1990). The two domains are hinged on one side so that the cleft opens and closes slightly on a picosecond time scale (Tirion & ben-Avraham, 1993) in a manner similar to the proposed "opened" to "closed" transitions of hexokinase and Hsc70 [see Holmes *et al.* (1993)]. In addition, time-resolved fluorescence energy transfer between the nucleotide and subdomain-2 of G-actin (Miki & Kouyama, 1994) shows a wide distribution of interprobe distances, indicating that structural flexibility and a large number of conformational substates exist in solution. The small orientation factor is consistent with these reports and suggests that the cleft of nucleotide-free actin in 48% sucrose may be closed a substantial fraction of the time.

ACKNOWLEDGMENT

We are extremely grateful to Fumio Oosawa for suggesting the use of sucrose to stabilize nucleotide-free actin from denaturation and to R. D. Mullins for performing preliminary experiments as a student in the physiology course at the Marine Biological Laboratory in Woods Hole. We thank E. M. Ostap, E. C. Petrella, and D. Shortle for suggestions on the manuscript and Lynn Selden for discussions on the constants in Scheme 1. We are particularly grateful to E. M. Ostap for offering much needed advice and suggestions throughout the course of this investigation and for his help with the kinetic simulations and experiments. We thank D. Shortle for use of the CD spectropolarimeter and J. Gillespie for his assistance, Peter Gillespie (Physiology) for use of the FPLC, and Tim Worrall (Middle Atlantic Mass Spectrometry Facility) for mass spectrometric analysis. We also thank A. S. Mildvan for his help in determining the interaction radius of ATP. E.M.D.L.C. thanks Drs. C. P. Reboulleau, H. H. Feder, and D. McCaslin for their continued support. We are grateful to an anonymous reviewer for informing us of the free calcium concentration in the preparation and for critical review of the manuscript and valuable suggestions.

REFERENCES

Anderson, N. G. (1970) in *CRC Handbook of Biochemistry, Selected Data for Molecular Biology* (Sober, H. A., Ed.) 2nd ed., pp J288–J291, CRC Press, Boca Raton, FL.

Asakura, S. (1961) *Arch. Biochem. Biophys. 92*, 140–149.

Berg, O. G., & von Hippel, P. H. (1985) *Annu. Rev. Biophys. Biophys. Chem. 14*, 131–160.

Bloembergen, N., & Morgan, L. O. (1961) *J. Chem. Phys. 34*, 842–850.

Cooper, J. A., & Pollard, T. D. (1982) *Methods Enzymol. 85*, 182–210.

Cotter, R. J. (1992) *Anal. Chem. 64*, 1027A–1039A.

Drewes, G., & Gaulstich, H. (1991) *J. Biol. Chem. 266*, 5508–5513.

Estes, J. E., Selden, L. A., Kinosian, H. J., & Gershman, L. C. (1992) *J. Muscle Res. Cell Motil. 13*, 272–284.

Faulstich, H., Merkler, I., Blackholm, H., & Stournaras, C. (1984) *Biochemistry 23*, 1608–1612.

Frieden, C., & Patane, K. (1988) *Biochemistry 27*, 3812–3820.

Gershman, L. C., Selden, L. A., & Estes, J. E. (1991) *J. Biol. Chem. 266*, 76–82.

Gerstein, M., Lesk, A. M., & Chothia, C. (1994) *Biochemistry 33*, 6739–6749.

Goldschmidt-Clermont, P., Machesky, L. M., Doberstein, S. K., & Pollard, T. D. (1991) *J. Cell Biol. 113*, 1081–1089.

Hegyi, G., & Venyaminov, S. Y. (1980) *FEBS Lett. 109*, 134–136.

Holmes, K. C., Sander, C., & Valencia, A. (1993) *Trends Cell Biol. 2*, 53–59.

Kabsch, W., Mannherz, H. G., Suck, D., Pai, E. F., & Holmes, K. C. (1990) *Nature 347*, 37–44.

Kasai, M., Nakano, E., & Oosawa, F. (1965) *Biochim. Biophys. Acta 94*, 494–503.

Kasprzak, A. A. (1993) *J. Biol. Chem. 268*, 13261–13266.

Kasprzak, A. A. (1994) *Biochemistry 33*, 12456–12462.

Kinosian, H. J., Selden, L. A., Estes, J. E., & Gershman, L. C. (1993) *J. Biol. Chem. 268*, 8683–8691.

Konno, K., & Morales, M. F. (1985) *Proc. Natl. Acad. Sci. U.S.A. 82*, 7904–7908.

Lanni, F., Taylor, D. L., & Ware, B. R. (1981) *Biophys. J. 35*, 351–364.

Lee, J. C., & Timasheff, S. N. (1981) *J. Biol. Chem. 256*, 7193–7201.

Lee, J. C., Frigon, R. P., & Timasheff, S. N. (1975) *Ann. N.Y. Acad. Sci. 253*, 284–291.

Lehrer, S. S., & Kerwar, G. (1972) *Biochemistry 11*, 1211–1217.

Mihashi, K. (1964) *Arch. Biochem. Biophys. 107*, 441–448.

Miki, M., & Kouyama, T. (1994) *Biochemistry 33*, 10171–10177.

Nagy, B., & Strzelecka-Golaszewska, H. (1972) *Arch. Biochem. Biophys. 150*, 428–435.

Neidl, C., & Engel, J. (1979) *Eur. J. Biochem. 101*, 163–169.

Nowak, E., & Goody, R. S. (1988) *Biochemistry 27*, 8613–8617.

Nowak, E., Strzelecka-Golaszewska, H., & Goody, R. S. (1988) *Biochemistry 27*, 1785–1792.

Pollard, T. D. (1984) *J. Cell Biol. 99*, 769–777.

Pollard, T. D., Goldberg, I., & Schwarz, W. H. (1992) *J. Biol. Chem. 267*, 20339–20345.

Press, W. H., Flannery, B. P., Teukolsky, S. A., & Vetterling, W. T. (1987) in *Numerical Recipes*, pp 550–560, Cambridge University Press, Cambridge, U.K.

Ralston, G. B. (1990) *J. Chem. Educ. 10*, 857–860.

Randerath, K., & Randerath, E. (1967) *Methods Enzymol. 12*, 323–347.

Sheterline, P., & Sparrow, J. C. (1993) *Protein Profile 1*, 1–125.

Shoham, M., & Steitz, T. A. (1980) *J. Mol. Biol. 140*, 1–14.

Sloan, D. L., & Mildvan, A. S. (1976) *J. Biol. Chem. 251*, 2412–2420.

Spudich, J. A., & Watt, S. (1971) *J. Biol. Chem. 246*, 4866–4871.

Strzelecka-Golaszewska, H., Venyaminov, S. Y., Zmorzynski, S., & Mossakowska, M. (1985) *Eur. J. Biochem. 147*, 331–342.

Tait, J. F., & Frieden, C. (1982) *Biochemistry 21*, 3666–3674.

Tirion, M. M., & ben-Avraham, D. (1993) *J. Mol. Biol. 230*, 186–195.

Tonomura, Y., & Yoshimura, J. (1961) *J. Biochem. 50*, 79–80.

Valentin-Ranc, C., & Carlier, M.-F. (1989) *J. Biol. Chem. 264*, 20871–20880.

Valentin-Ranc, C., & Carlier, M.-F. (1991) *J. Biol. Chem. 266*, 7668–7675.

von Hippel, P. H., & Berg, O. G. (1989) *J. Biol. Chem. 264*, 675–678.

Wachsstock, D. H., & Pollard, T. D. (1994) *Biophys. J. 67*, 1260–1273.

Waechter, F., & Engel, J. (1975) *Eur. J. Biochem. 57*, 453–459.

Waechter, F., & Engel, J. (1977) *Eur. J. Biochem. 74*, 227–232.

Winzor, D. J., & Wills, P. R. (1986) *Biophys. Chem. 25*, 243–251.

BI942587Y